RESEARCH ARTICLE

# Asiatic Acid Modulates *Il6* and *Tgfb1* mRNA Expression and Soluble Collagen Levels in RAW 264.7–NIH 3T3 Co-culture Cells under High-Glucose and LPS Stimulation

Rizki Awaluddin[1,*], Dwi Aris Agung Nugrahaningsih[2], Eti Nurwening Sholikhah[2], Hermanus Ehe Hurit[1]

[1]Program Studi Farmasi, Fakultas Ilmu-ilmu Kesehatan, Universitas Esa Unggul, Jl. Arjuna Utara No. 9. Jakarta 11510, Indonesia
[2]Department of Pharmacology and Therapy, Faculty of Medicine, Public Health, and Nursing, Universitas Gadjah Mada, Jl. Farmako Sekip Utara, Yogyakarta 55281, Indonesia

*Corresponding author. Email: rizki.awaluddin@esaunggul.ac.id

Received date: Jul 8, 2026; Revised date: Aug 15, 2026; Accepted date: Aug 20, 2026

## Abstract

**BACKGROUND:** Chronic inflammation contributes to diabetes-associated fibrosis, through persistent hyperglycemia, leading to increased interleukin-6 (IL-6), transforming growth factor-β (TGF-β), and collagen levels. While metformin effectively controls blood glucose, it may not adequately suppress these pathogenic pathways. Asiatic acid has demonstrated anti-inflammatory and antifibrotic properties, although its effects within a direct-contact macrophage–fibroblast microenvironment such as in co-culture models remain unclear. This study was conducted to evaluate the effects of asiatic acid on *Il6*, *Tgfb1*, and soluble collagen levels in a RAW 264.7–NIH 3T3 co-culture under high-glucose and lipopolysaccharide (HG–LPS) stimulation.

**METHODS:** RAW 264.7 and NIH 3T3 cells were co-cultured at ratios of 1:1–1:6, and the selected co-culture was treated with asiatic acid (2.5, 5.0, and 10.0 µg/mL) for 24 h while HG–LPS stimulation was maintained. Unstimulated NIH 3T3 monocultures and untreated HG–LPS co-cultures served as controls. The inflammatory and profibrotic markers such as *Il6* and *Tgfb1* mRNA expression were quantified by polymerase chain reaction (PCR), and soluble collagen was measured using a modified Sirius Red assay.

**RESULTS:** Among the tested ratios, the 1:1 co-culture exhibited the highest *Tgfb1* mRNA expression (0.35±0.02) and soluble collagen level (1.30±0.00) and was selected for subsequent experiments, whereas *Il6* mRNA expression did not differ significantly among co-culture ratios. Under HG–LPS stimulation, *Il6* and *Tgfb1* mRNA expression increased 3.5-fold and 10.3-fold, respectively, compared with unstimulated NIH 3T3 monocultures. Asiatic acid significantly reduced *Il6* mRNA expression at 5.0 and 10.0 µg/mL, *Tgfb1* mRNA expression at 2.5 µg/mL, and soluble collagen levels at all tested concentrations, indicating a non-monotonic concentration–response pattern.

**CONCLUSION:** The 1:1 RAW 264.7–NIH 3T3 co-culture was the most responsive under HG–LPS stimulation and could be *in vitro* platform for investigating macrophage–fibroblast interactions under hyperglycemic inflammatory conditions. Asiatic acid modulated *Il6* and *Tgfb1* mRNA expression and soluble collagen levels in RAW 264.7–NIH 3T3 co-culture, which suggest that Asiatic acid may be potential for the management of fibrotic inflammation.

**KEYWORDS:** co-culture, collagen, fibroblast dysfunction, NIH 3T3 fibroblast, RAW 264.7 macrophage

***Indones Biomed J. 2026; 18(4): 397-406***

## Introduction

The efficacy of anti-diabetic drugs to controlling diabetic blood glucose has been established. However, inadequate therapy may cause tissue injury. Inadequate management of Type 2 Diabetes Mellitus (T2DM) is associated with elevated pro-inflammatory cytokines to induce chronic inflammation, and increased pro-fibrotic factors. Fibrosis can occur in multiple organs in diabetic conditions. Previous study reported that diabetic condition associated with worse outcome in Idiopathic Pulmonary Fibrosis (IPF) there are have a higher hospital stay length and mortality rate.(1,2)

Fibrosis is a key factor in diabetic complications, contributing to dysfunction in the kidneys, liver, and heart, such as renal fibrosis as diabetic nephropathy, hepatic fibrosis and myocardial remodeling.(3–5) These conditions are associated with prolonged hyperglycemia, which leads to the activation of proinflammatory macrophages. (6) The secretion of proinflammatory cytokines, such as interleukin (IL)-6, induces cellular stress and fibroblast dysfunction, resulting in the overexpression of transforming growth factor-β (TGF-β) and excessive extracellular matrix deposition characterized with collagen secretion. (7) Although metformin remains the first-line therapy for T2DM and has demonstrated beneficial clinical outcomes, diabetic complications are characterized by complex inflammatory and profibrotic pathways that extend beyond glycemic dysregulation.(8) Previous study reported that metformin reduce 18% risk of hospitalization and 54% reduction in all-cause mortality in T2DM with IPF.(9) Diabetic complication involve complex inflammatory and profibrotic pathways that may require therapeutic approach beyond glycemic control. Therefore, alternative therapeutic strategies capable of suppressing inflammation and fibrosis are needed to address diabetic complications.

Asiatic acid from *Centella asiatica* has been shown to attenuate pro-inflammatory cytokine and TGF-β secretion in macrophages.(10) Previous studies showed that 25 mg/kg BW asiatic acid alleviates hyperglycemia and reduces islet fibrosis in Goto–Kakizaki rats.(11) Although asiatic acid effect on TGF-β have been confirmed in both *in vivo* and *in vitro* studies, *in vivo* approaches are inherently complex and limited in their ability to delineate the specific roles of fibroblasts and macrophages during fibrosis.(12) Conversely, *in vitro* monoculture models of fibroblasts and/or macrophages, whether through direct exposure or conditioned media, primarily represent unidirectional interactions and lack the tissue microenvironment (TME), which remains a major limitation of these systems.(13)

The co-culture model can demonstrate capture macrophage–fibroblast crosstalk through both paracrine and juxtacrine interactions.(14,15) However, direct-contact macrophage–fibroblast co-culture models under hyperglycemic and pro-inflammatory conditions remain limited, and the effects of asiatic acid in this setting are unclear. Therefore, this study was condted to identify the most responsive RAW 264.7–NIH 3T3 co-culture ratio under high-glucose and LPS (HG–LPS) stimulation and evaluated the effects of asiatic acid on *Il6* and *Tgfb1* mRNA expression and soluble collagen levels.

## Methods

### Cell Culture

RAW 264.7 macrophages (ATCC® TIB-71; ATCC, Manassas, VA, USA) and NIH 3T3 fibroblasts (ATCC® CRL-1658; ATCC) passage-122 were obtained from the Department of Biological Science and Technology, National Pingtung University of Science and Technology (NPUST, Pingtung, Taiwan). The cell culture was maintained in DMEM (Gibco® 12800-058; Thermo Fisher Scientific, Waltham, MA, USA) containing 2% penicillin–streptomycin and 10% fetal bovine serum (FBS) (Gibco® 26140-079; Thermo Fisher Scientific), and then incubated at 37°C with 5% $CO_2$. RAW 264.7 and NIH 3T3 were maintained routinely in T-25 flask at 500,000 cells and subcultured every two days.

### Co-culture of RAW 264.7 Macrophage Cells and NIH 3T3 Fibroblast Cells

Optimization of co-culture models were conducted with RAW 264.7 and NIH 3T3 cells were co-seeded at ratios of 1:1–1:6 in 6-well plates (Table 1). The initial seeding number for each cell type was calculated from the projected cell number after 72 h using the exponential growth equation:

$$N_0 = \frac{N_t}{2^{t/DT}}$$

Where $N_0$ is the initial number of seeded cells, $N_t$ is the projected cell number after 72 h, while t is the incubation time (72 h), and DT is the experimentally determined doubling time of each cell line.

The doubling times of RAW 264.7 and NIH 3T3 cells were experimentally determined from routine growth-curve

**Table 1. Initial cell seeding density used for each experimental group and the estimated cell number after 72 h of culture.**

| Group | Cell type | Initial Cell Seeding Density (Cells/well) | Estimated Cell Number After 72 h (Cells/well) |
|---|---|---|---|
| Unstimulated | NIH 3T3 | 22.696 | 1.000.000 |
| HG-LPS | NIH 3T3 | 22.696 | 1.000.000 |
| Co-culture 1:1 | RAW 264.7 | 22.696 | 1.000.000 |
| | NIH 3T3 | 324.990 | 1.000.000 |
| Co-culture 1:2 | RAW 264.7 | 11.348 | 500.000 |
| | NIH 3T3 | 324.990 | 1.000.000 |
| Co-culture 1:3 | RAW 264.7 | 7.565 | 333.333 |
| | NIH 3T3 | 324.990 | 1.000.000 |
| Co-culture 1:4 | RAW 264.7 | 5.674 | 250.000 |
| | NIH 3T3 | 324.990 | 1.000.000 |
| Co-culture 1:5 | RAW 264.7 | 4.539 | 200.000 |
| | NIH 3T3 | 324.990 | 1.000.000 |
| Co-culture 1:6 | RAW 264.7 | 3.783 | 166.667 |
| | NIH 3T3 | 324.990 | 1.000.000 |

analyses under standard DMEM culture conditions and were approximately 13.2 h and 44.4 h, respectively. The RAW 264.7 and NIH 3T3 cells were seeded together in the same well for 24 h in standard DMEM (containing 4500 µg/mL glucose) and incubated at 37°C and 5% $CO_2$. After the initial 24 h incubation, co-cultures were stimulated with 0.25 µg/mL LPS and additional D-glucose supplementation to achieve a final glucose concentration of 5400 µg/mL in DMEM supplemented with 10% FBS for 48 h (hereafter referred to as HG-LPS condition). For comparison, NIH 3T3 monocultures were cultured under identical conditions either without stimulation (unstimulated control) or following stimulation with HG-LPS medium (HG-LPS control). The co-culture optimization experiments were performed using two independent biological replicates. Subsequently, cells and culture media were collected to assess *Il6* and *Tgfb1* mRNA expression, as well as collagen levels.

The most responsive ratio was selected for subsequent experiments. Cells were co-cultured under the same conditions and stimulated with LPS and high glucose for 24 h, followed by treatment with asiatic acid (2.5, 5.0, and 10.0 µg/mL) for an additional 24 h under identical conditions. The asiatic acid treatment experiments were performed using three independent biological replicates. Culture supernatants were stored at −20°C, and cells were harvested for RNA isolation.

**Quantification of Soluble Collagen Levels in Culture Medium**

Collagen levels in the culture medium were quantified using a modified Sirius Red assay. Collagen was precipitated with polyethylene glycol 400 overnight and the resulting pellet was dissolved in 0.1 M acetic acid. Type I collagen from rat tail (Sigma-Aldrich C7661-5MG; Sigma-Aldrich, St. Louis, MO, USA) served as the standard, with DMEM as the medium control and 0.1 M acetic acid as the solvent control. Fifty µL of samples were mixed with 250 µL of 1% Sirius Red solution and incubated at room temperature for 20 min to allow collagen precipitation. Excess dye was removed using 0.1 N HCl, followed by dissolution of the pellet in 0.5 M NaOH (150 µL). The solution was transferred to a 96-well plate, and absorbance was measured at 540 nm. The absorbance values were corrected by subtracting the vehicle control absorbance. Soluble collagen concentrations (µg/mL) were subsequently calculated by extrapolation from the linear regression equation of the Type I collagen standard curve. The collagen assay was performed using three independent biological replicates. Soluble collagen concentrations were expressed as µg/mL.(16)

**RNA Isolation and Polymerase Chain Reaction (PCR) Analysis**

Total RNA from control and treated cells was extracted using Tri-RNA reagent. Total RNA concentration and purity

were assessed spectrophotometrically using a NanoDrop Lite spectrophotometer (Thermo Fisher Scientific) by measuring absorbance at 260/280 nm ratio.(17) Reverse transcription was performed using 100 ng/µL RNA, mixed with ExcelRT™ Reverse Transcription Kit II (Smobio RP1400; SMOBIO Technology, Hsinchu City, Taiwan), and thermal cycler were set at 25°C for 11 min, 42°C for 50 min, and 85°C for 5 min. PCR amplification was carried out using 1 µL of cDNA with gene-specific primers for *Il6* (forward: 5′-ACTGATGCTGGTGACAACCACG-3′; reverse: 5′-AGCCTCCGACTTGTGAAGTGG-3′), *Tgfb1* (forward: 5′-TTCCGCTGCTACTGCAAGTCA-3′; reverse: 5′-GGGTAGCGATCGAGTGTCCA-3′), and *Gapdh* (forward: 5′-TGTGTCCGTCGTGGATCTGA-3′; reverse: 5′-TTGCTGTTGAAGTCGCAGGAG-3′). The primers were designed using Primer-BLAST and synthesized commercially. Primer specificity was confirmed by the appearance of a single amplicon band in RT-PCR analysis. *Il6* and *Tgfb1* mRNA expressions were quantified by reverse transcription PCR (RT-PCR) and quantitative real-time PCR (qRT-PCR) using *Gapdh* as the internal reference gene.

RT-PCR was used to evaluate *Il6* and *Tgfb1* mRNA expression in the optimized co-culture model using GoTaq® Green Master Mix (Promega M7122; Promega Corporation, Madison, WI, USA). Amplification was performed for 35 cycles under the following conditions: initial denaturation at 95°C for 7 min; annealing at 60°C (*Gapdh*), 62°C (*Il6*), and 54°C (*Tgfb1*) for 1 min; and extension at 72°C for 4 min 45 s. All reactions were carried out in duplicate. PCR products were separated on 2% agarose gels, stained with FluoroVue™ nucleic acid stain, and quantified by densitometry using ImageJ (National Institutes for Health, Bethesda, MD, USA).

qRT-PCR was performed using ExcelTaq™ 2× Fast Q-PCR Master Mix (SYBR, ROX) on a C1000 Thermal Cycler CFX96™ system (Bio-Rad, Hercules, CA, USA). The reactions were run for 40 cycles under the following conditions: pre-denaturation at 95°C for 1 min, denaturation at 95°C for 30 s, and annealing at 62°C (Il6) and 55.3°C (Tgfb1) for 30 s. Melt-curve analysis was performed for each qRT-PCR assay to assess amplification specificity, and the corresponding no-template controls (NTCs) were evaluated for nonspecific amplification. Each biological sample was analyzed in technical duplicate, and relative gene expression was calculated using the $2^{-\Delta\Delta Cq}$ method.(18)

### Statistical Analysis

Data on *Il6* and *Tgfb1* mRNA expression and collagen levels were presented as mean±standard deviation (SD). Data normality was assessed using the Shapiro–Wilk test. Normally distributed data were analyzed using one-way ANOVA followed by Tukey's multiple comparison test. Differences were considered statistically significant at $p<0.05$ and $p<0.01$.

## Results

### Optimization of RAW 264.7–NIH 3T3 Co-culture Ratio in HG-LPS Condition

In order to find the most responsive direct contact co-culture ratio for a diabetes mellitus *in vitro* model. The *Il6* and *Tgfb1* mRNA expressions, and collagen secretion were evaluated in various ratio of RAW 264.7 and NIH 3T3 co-culture cells.

#### *Il6 mRNA Expression*

Based on the analysis of *Il6* mRNA expression (Figure 1), co-culture cells cultured under HG-LPS conditions exhibited higher *Il6* mRNA expression than NIH 3T3 monoculture cells cultured under HG-LPS conditions (1.23±0.01 *vs.* 1.03±0.04, $p=0.024$). However, no statistically significant differences were observed compared with the other experimental groups.

#### *Tgfb1 mRNA Expression*

As shown in Figure 2, *Tgfb1* mRNA expression was significantly higher in the 1:1 and 1:3 co-culture groups than in the NIH 3T3 monoculture unstimulated (0.35±0.02 and 0.34±0.00 *vs.* 0.18±0.04, $p=0.019$ and $p=0.031$) and HG-LPS conditions (*vs.* 0.14±0.01, $p=0.006$ and $p=0.009$). In contrast, *Tgfb1* mRNA expression in the 1:5 and 1:6 co-

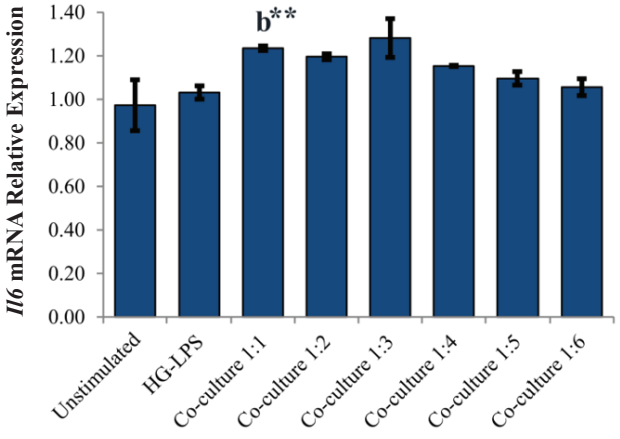


**Figure 1. The *Il6* mRNA expressions in variation of RAW 264.7–NIH 3T3 co-culture ratio in HG-LPS conditions.** Statistical significance: *$p<0.05$, **$p<0.01$ with a (*vs.* Unstimulated), b (*vs.* HG-LPS), c (*vs.* Co-culture 1:1), n=2.

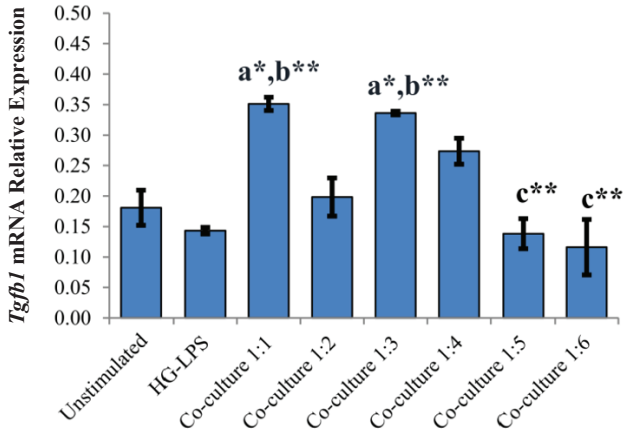


**Figure 2. The *Tgfb1* mRNA expressions in variation of RAW 264.7–NIH 3T3 co-culture ratio in HG-LPS conditions.** Statistical significance: *$p$<0.05, **$p$<0.01 with a (*vs.* Unstimulated), b (*vs.* HG-LPS), c (*vs.* Co-culture 1:1), n=2.

culture groups was significantly lower than that in the 1:1 co-culture group (0.14±0.03 and 0.12±0.06 *vs.* 0.35±0.02, $p$=0.005 and $p$=0.003).

***Soluble Collagen Level***

As shown in Figure 3, the 1:1 co-culture group exhibited the highest relative collagen level (1.30±0.00) among all groups. However, statistical significance was observed only when compared with the 1:5 and 1:6 co-culture groups (0.56±0.03 and 0.53±0.02, $p$=0.031 and $p$=0.025).

**Effect of Asiatic Acid on the Optimized Co-culture Model in HG-LPS Condition**

To understand asiatic acid effects on inflammation and collagen secretion, we investigated *Il6* and *Tgfb1* mRNA expression, and collagen level in a optimized co-culture (1:1) of RAW 264.7 and NIH 3T3 cells induced HG-LPS medium after treated with various concentrations of Asiatic acid (2.5, 5.0, and 10.0 µg/mL) for 24 h.

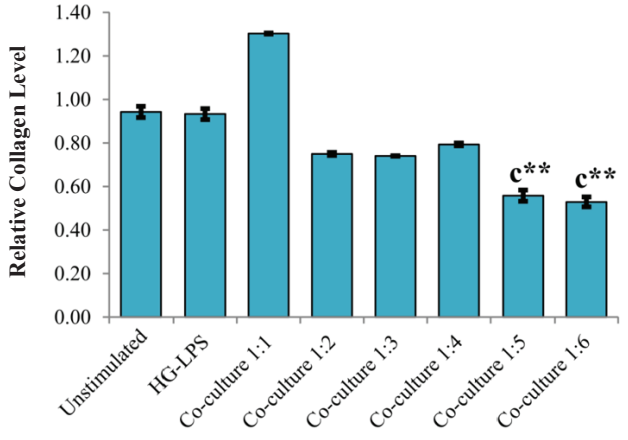


**Figure 3. The relative soluble collagen level (OD sample/OD medium control) in variation of RAW 264.7–NIH 3T3 co-culture ratio in HG-LPS conditions.** Statistical significance: *$p$<0.05, **$p$<0.01 with a (*vs.* Unstimulated), b (*vs.* HG-LPS), c (*vs.* Co-culture 1:1), n=2.

***Il6 mRNA Expression***

As shown in Figure 4, the *Il6* mRNA expression on a co-culture cell was significantly higher 3.5 fold compared with unstimulated NIH 3T3 monoculture (3.54±0.94 *vs.* 1.05±0.44, $p$=0.002). The asiatic acid attenuates *Il6* mRNA expression. The *Il6* mRNA expression in co-culture cells treated asiatic acid (5.0 and 10.0 µg/mL) were lower significantly ($p$<0.05) than co-culture cells (2.77±0.53, $p$=0.029 and 1.66±0.053, $p$=0.016 *vs.* 3.54±0.94). Melt-curve analysis of the *Il6* assay (Supplementary 1) showed a single peak for both *Il6* and *Gapdh*, with melting temperatures (Tm) of 80.5°C and 83.0°C, respectively. No amplification peak was observed in the corresponding NTCs.

***Tgfb1 mRNA Expression***

As shown in Figure 5, *Tgfb1* mRNA expression was significantly higher 10.3 fold in the co-culture group than in unstimulated NIH 3T3 monoculture (10.3±0.63 *vs.* 1.03±0.28, $p$=0.001). Treatment with asiatic acid modulated *Tgfb1* mRNA expression in the co-culture cells. Specifically, asiatic acid at 2.5 µg/mL significantly reduced *Tgfb1* mRNA expression compared with the co-culture group (7.77±0.89 *vs.* 10.3±0.63, $p$=0.009). In contrast, treatment with 5.0 µg/mL resulted in a higher *Tgfb1* mRNA expression than the co-culture group, whereas treatment with 10.0 µg/mL resulted in a lower expression; however, neither difference was statistically significant. Melt-curve analysis of the *Tgfb1* assay (Supplementary 2) showed a single peak for both *Tgfb1* and *Gapdh*, with Tm of 84.5°C and 83.0°C, respectively. No amplification peak was observed in the *Tgfb1* NTC, whereas minor amplification was observed in the *Gapdh* NTC at a melting temperature distinct from that of the Gapdh amplicon.

***Soluble Collagen Level***

As shown in Figure 6, the collagen level on a co-culture cell were higher significantly ($p$<0.01) compared with unstimulated NIH 3T3 monoculture (104.67±35.05 *vs.* 19.04±5.01, $p$=0.001). Collagen levels showed a lower significantly difference following exposure to all concentrations of asiatic acid compared with the co-culture cell group, despite exhibiting an inverse concentration-dependent (43.21±8.53; 52.17±1.57; and 58.21±1.57 *vs.* 104.67±35.05, $p$=0.007; 0.018; and 0.037, respectively).

Direct-contact co-culture under HG–LPS–induced conditions and exposure to asiatic acid affected the

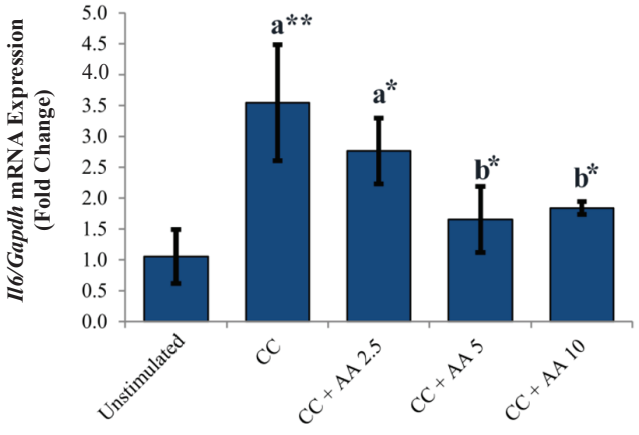


**Figure 4. Effects of asiatic acid on *Il6* mRNA expression in RAW 264.7–NIH 3T3 co-culture 1:1.** Data are presented as mean±SD from three independent experiments. Statistical significance: **p*<0.05, ***p*<0.01 with a (*vs.* Unstimulated), b (*vs.* CC), n=3. CC: co-culture cell; AA: asiatic acid.

microscopic morphology of the cells. As shown in Figure 7A, NIH 3T3 cells in monoculture exhibited a large, elongated, and irregular (stellate-like) morphology, whereas NIH 3T3 cells in co-culture displayed smaller, spindle-shaped and elongated morphologies. In contrast, macrophages showed prominent pseudopodia and irregular shapes (Figure 7B). Furthermore, in co-cultured cells treated with asiatic acid, NIH 3T3 cells exhibited irregular morphologies, accompanied by an increased number of round-shaped RAW 264.7 cells. However, visual observation revealed no marked morphological differences among the various concentrations of asiatic acid (Figure 7C–7E).

## Discussion

High glucose in this study play role to reproduce the hyperglycemic stress metabolic associated with diabetes, whereas LPS promotes inflammatory stress to activate macrophage and enhance macrophage-fibroblast crosstalk. (19) The combined stimulation was intended to establish a hyperglycemic inflammatory microenvironment condition that mimics selected inflammatory features associated with diabetic complication. As shown in Figure 1 and Figure 2, *Il6* and *Tgfb1* mRNA expression in co-culture cells is higher than in unstimulated NIH 3T3 monoculture. HS-LPS tended to increase *Il6* expression; however, the difference was not statistically significant. Hyperglycemia has been reported to activate macrophage cells to amplify Toll-like receptors and secrete proinflammatory cytokines.(20,21) Proinflammatory macrophages release various mediators, including cytokines, chemokines, and growth factors (22,23), which can promote excessive collagen production in fibroblasts, particularly in idiopathic pulmonary fibrosis.(24) Direct macrophage–fibroblast co-culture further enhances signaling via autocrine and paracrine interactions.(25). Although *Il6* expression also tended to be higher in the 1:1 co-culture, the differences among co-culture ratios were not statistically significant. Previous studies have suggested that combined HS-LPS stimulation may increase soluble collagen levels, potentially reflecting enhanced inflammatory and profibrotic mediator in the mixed-cell system.(26) In this study, LPS and high-glucose stimulation increased *Il6* mRNA expression more

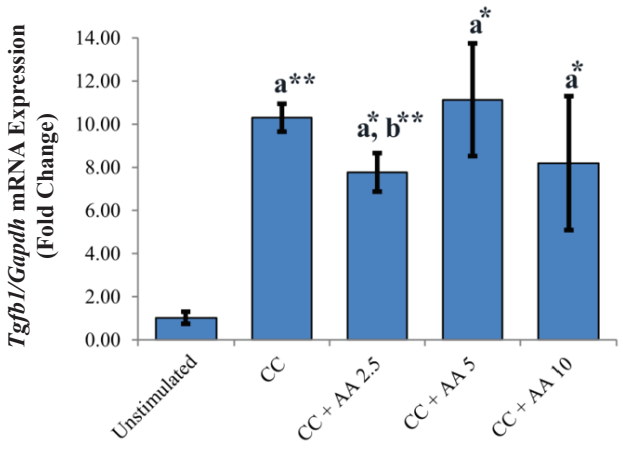


**Figure 5. Effects of asiatic acid on *Tgfb1* mRNA expression in RAW 264.7–NIH 3T3 co-culture 1:1.** Data are presented as mean±SD from three independent experiments. Statistical significance: **p*<0.05, ***p*<0.01 with a (*vs.* Unstimulated), b (*vs.* CC), n=3. CC: co-culture cell; AA: asiatic acid.

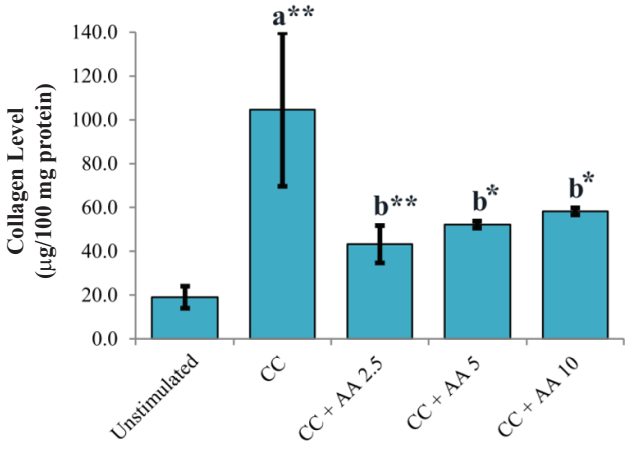


**Figure 6. Effects of asiatic acid on collagen levels in RAW 264.7–NIH 3T3 co-culture 1:1.** Data are presented as mean±SD from three independent experiments. Statistical significance: **p*<0.05, ***p*<0.01 with a (*vs.* Unstimulated), b (*vs.* CC), n=3. CC: co-culture cell; AA: asiatic acid.

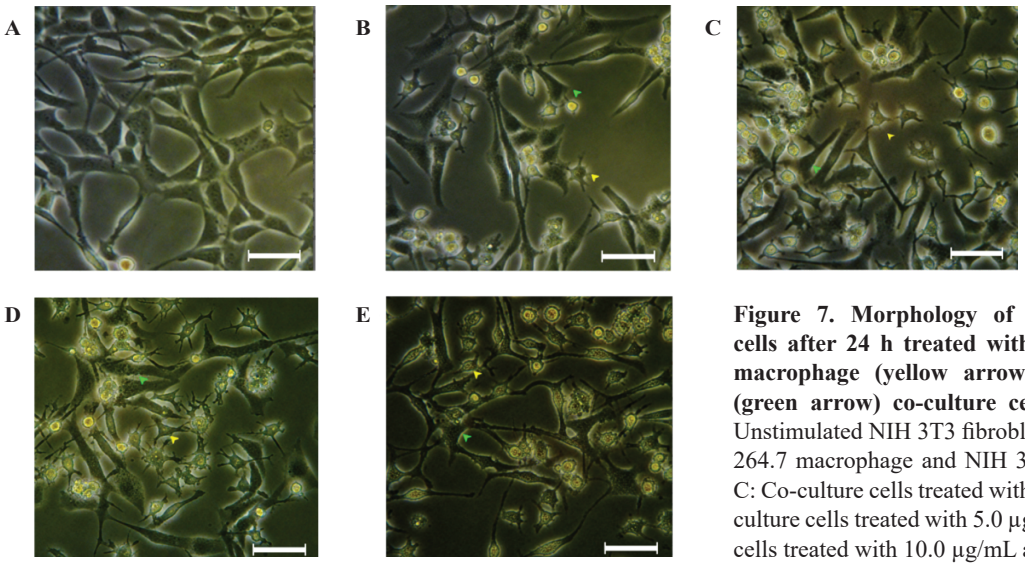


**Figure 7. Morphology of macrophage and fibroblast cells after 24 h treated with asiatic acid on RAW 264.7 macrophage (yellow arrow) and NIH 3T3 Fibroblast (green arrow) co-culture cells in HG-LPS medium.** A: Unstimulated NIH 3T3 fibroblast monoculture cells. B: RAW 264.7 macrophage and NIH 3T3 Fibroblast co-culture cells. C: Co-culture cells treated with 2.5 µg/mL asiatic acid. D: Co-culture cells treated with 5.0 µg/mL asiatic acid. E: Co-culture cells treated with 10.0 µg/mL asiatic acid . White bar: 50 µm.

prominently in RAW 264.7–NIH 3T3 co-cultures than in NIH 3T3 monocultures. These findings are consistent with previous studies suggesting that HG-LPS stimulation may promote inflammatory responses trough mitochondrial oxidative stress and Toll-like receptor 4 (TLR4) signaling, despite this pathways were note evaluated in the present study.(27,28)

The *in vitro* direct-contact co-culture model was used to investigate macrophage-fibroblast interactions under hyperglycemic inflammatory conditions. The co-culture cells RAW 264.7 and NIH 3T3 under conditions of LPS and high glucose were also associated with hypersecretion of collagen, which may be associated with enhanced profibrotic signaling, including TGF-β related pathways reported in previous studies. The previous research reported that pro-inflammatory macrophages induce expression of type-1 and type-3 collagen genes in human skin fibroblast cells cultured in LPS-induced macrophage-conditioned media. Fibroblast cells have IL-6 and TGF-β transmembrane receptors on the surface, which were associated with inflammatory mediators produced by macrophage.(29)

The current findings demonstrate that varying the RAW 264.7–NIH 3T3 cell ratio influenced *Tgfb1* mRNA expression and soluble collagen levels, whereas *Il6* mRNA expression showed no statistically significant differences among the tested co-culture ratios. The 1:1 ratio was selected for subsequent experiments because it exhibited the highest *Tgfb1* mRNA expression and soluble collagen level among the tested ratios. These differences may reflect altered macrophage–fibroblast interactions resulting from different cell ratios. According to previous studies, TGF-β signaling may be enhanced through autocrine and paracrine mechanisms and proceeds via both Smad-dependent and Smad-independent pathways.(30) In the Smad-dependent pathway, TGF-β receptor activation promotes Smad2/3–Smad4 complex formation, leading to transcription of collagen-related genes. Alternatively, Smad-independent signaling may involve mitogen-activated protein kinase (MAPK) pathways, including extracellular signal-regulated kinase (ERK), p38, and c-Jun N-terminal kinase (JNK) which can also regulate activator protein-1 (AP-1) activity and extracellular matrix production. This hypothesis provides possible mechanism that may explain increased *Tgfb1* expression and soluble collagen levels observed in the HG-LPS stimulated co-culture model, although these signaling pathways were not directly investigated in the present study and needs to be validated in further studies. (31)

The results of current study revealed that asiatic acid modulated inflammatory and profibrotic markers in the co-cuture model. Significant reduction in *Tgfb1* mRNA expression and soluble collagen levels were observed. However, overall responses across concentrations were non-monotonic rather than concentration dependent. TGF-β is a pleiotropic cytokine with immunoregulatory function and a well-established role as a key profibrotic mediator. (32) Asiatic acid may attenuate inflammatory signaling and thereby reduce extracelluar matrix remodeling in the co-culture model.(33) Asiatic acid alleviates inflammation in RAW 264.7 cells via inhibition of nuclear factor-kappaB (NF-κB) and Notch signaling pathways.(34) Previous studies suggest that inhibition of NF-κB and Notch

signaling may attenuate inflammatory signaling, which could contribute to the reduce *Il6* expression observed in the co-culture system. Another study reported that Asiatic acid inhibit collagen secretion by suppress of signal transducer and activator of transcription 3 (STAT3) pathway activation.(35) These pathway may contribute to the observed reduction in soluble collagen levels, although STAT3 was not examined in the present study. However, the changes in *Il6* mRNA expression were not consistently accompanied by similar changes in *Tgfb1* mRNA expression or soluble collagen levels across the tested asiatic acid concentrations, suggesting that *Il6* alone may not fully explain the profibrotic response observed in this model. Evidence from previous studies indicates that TGF-β expression is regulated by multiple pro-inflammatory cytokines, including IL-1β, TNF-α, and IL-6, together with other signaling pathways involved in tissue remodeling. Therefore, the differential response patterns observed in the present study may reflect the complex regulation of inflammatory and profibrotic signaling rather than a direct relationship between *Il6* expression and downstream fibrotic markers.(36)

Current findings showed that reduction in soluble collagen levels did not consistently parallel the changes in *Tgfb1* expression, suggesting that collagen production may be regulated by multiple pathways beyond TGF-β alone. Previous studies have implicated both Smad-dependent and non-Smad signaling, including MAPK, JNK, p38, IKK, and phosphoinositide 3-kinase (PI3K) pathways, in the regulation of collagen production.(37,38) These pathways may represent alternative mechanisms underlying the collagen response observed in the present study, although they were not directly investigated.

As shown in Figure 7C-7E, morphological observations also revealed cell shrinkage, cytoplasmic condensation, and reduced cell density in the co-culture treated with 10 µg/mL asiatic acid, which may indicate cytotoxicity or apoptosis. However, cell viability was not directly evaluated in this HG-LPS medium. In our previous study, asiatic acid at concentrations of 3.125–12.5 µg/mL maintained >80% viability in RAW 264.7 and NIH 3T3 monocultures under standard culture conditions, with $IC_{50}$ values of 15.21 and 18.95 µg/mL, respectively.(39) Nevertheless, because cell viability was not reassessed under HG–LPS-stimulated co-culture conditions, the contribution of cytotoxicity to the observed reductions in *Il6*, *Tgfb1*, and soluble collagen levels cannot be completely excluded. Previous research has shown that asiatic acid can induce apoptosis via several signaling pathways, including TGF-β/Yes-associated protein (YAP)-mediated signaling and the modulation of B-cell lymphoma 2 (Bcl-2), Bcl-2-associated X protein (Bax), and Bcl-xL expression.(40) However, these pathways were not investigated in the current study and should therefore be considered potential mechanistic hypotheses rather than confirmed mechanisms. Our findings indicate that asiatic acid modulated *Il6*, *Tgfb1*, and soluble collagen levels in the macrophage–fibroblast co-culture model, despite the response was non-monotonic rather than concentration-dependent. Such variable responses across concentrations may reflect the complexity of inflammatory and profibrotic signaling networks or differences in cellular responses within the direct-contact co-culture system.

The findings of this study have limitations there are that could be addressed in future research. First, RNA and soluble collagen were obtained from direct-contact co-cultures. Therefore, the relative contribution of RAW 264.7 macrophages and NIH 3T3 fibroblasts to *Il6*, *Tgfb1*, and soluble collagen production could not be distinguished. Second, the experimental design did not include unstimulated co-culture, LPS-only, or high-glucose-only control groups. Inclusion of these controls would facilitate the evaluation of the independent and combined effects of hyperglycemia and inflammatory stimulation on the co-culture model. Furthermore, information regarding passage history, cell-line authentication, and mycoplasma testing was unavailable for the cell stocks obtained from the collaborating institution. Finally, amplification efficiency could not be retrospectively determined because no serial-dilution standard curve was performed, although melt-curve analysis and corresponding no-template controls were evaluated to assess amplification specificity.

## Conclusion

Among the tested direct-contact RAW 264.7–NIH 3T3 co-culture ratios, the 1:1 ratio was the most responsive within an HG–LPS-induced hyperglycemic inflammatory microenvironment, and might be used as a responsive in vitro platform for investigating macrophage–fibroblast interactions and pharmacological responses under hyperglycemic inflammatory conditions. Asiatic acid modulated Il6 mRNA expression, Tgfb1 mRNA expression, and soluble collagen levels in RAW 264.7–NIH 3T3 co-culture, with a non-monotonic concentration-response pattern. These findings suggest that Asiatic acid might be potential for the management of fibrotic inflammation.

## Acknowledgments

The author thanks the Directorate General of Higher Education, Research and Technology for the international scientific articles writing program.

## Authors Contribution

RA and DAAN were involved in the Conceptualization. RA prepared the methodology and software. DAAN and ENS performed the validation. RA and HEH performed formal analysis. RA performed investigation. RA and DAAN prepared the resources. DAAN and ENS performed data curation. RA and HEH prepared original draft preparation, as well as reviewing and editing the manuscript. RA prepared the visualization. DAAN and ENS supervised the study. DAAN was responsible for the project administration and funding acquisition. All authors have gave final approval for the manuscript before submission.

## Ethical Statement

This study was conducted in accordance with institutional requirements for biomedical research and under an institutional research protocol reviewed and approved by the Medical and Health Research Ethics Committee (MHREC) of the Faculty of Medicine, Public Health, and Nursing, Universitas Gadjah Mada (No. KE/FK/0878/EC/2018).

## Conflict of Interest

The authors declare that they have no competing interests.

## References

1. Wang D, Ma Y, Tong X, Zhang Y, Fan H. Diabetes mellitus contributes to idiopathic pulmonary fibrosis: A review from clinical appearance to possible pathogenesis. Front Public Health. 2020; 8: 196. doi: 10.3389/fpubh.2020.00196.
2. Kanasaki K, Taduri G, Koya D. Diabetic nephropathy: The role of inflammation in fibroblast activation and kidney fibrosis. Front Endocrinol. 2013; 4: 7. doi: 10.3389/fendo.2013.00007.
3. Erimşah S, Çetinkaya A, Üyetürk Ü, Üyetürk U, Yazır Y. The antioxidant effects of sesamol on bleomycin-induced oral submucous fibrosis. Experimed. 2022; 12: 238–42.
4. Terasaka Y, Takahashi H, Amano K, Fujisaki K, Kita S, Kato K, *et al.* Change in liver fibrosis associates with progress of diabetic nephropathy in patients with nonalcoholic fatty liver disease. Nutrients. 2023; 15(4): 3248. doi: 10.3390/nu15143248.
5. Kirtaniya AAIK, Lestarini A, Permatananda PANK, Aryastuti AASA. Association of ELMO1 genetic polymorphism (rs741301) with the progression of diabetic kidney disease in Balinese patients with type 2 diabetes mellitus. Mol Cell Biomed Sci. 2023; 7(1): 47–51.
6. Venkatesan K, Paulsamy P, Alqahtani S, Asiri YI, Alqahtani T, Alqahtani A, *et al.* An update on the role of inflammation in insulin resistance and islet β cell failure - A crosstalk between immune cells, adipose tissue, cytokines, and oxidative stress. Lett Drug Des Discov. 2025; 22(3): 100023. doi: 10.1016/j.lddd.2025.100023.
7. Jayaraman J, Namsivayam N, Manivannan K, Sundaresan U. Therapeutic effect of naringenin on ethanol-induced liver fibrosis in rats. Eur J Clin Exp Med. 2025; 23(3): 626–32.
8. Massen GM, Cook S, Moss ST, Chambers R, Jenkins G, Allen RJ, *et al.* Association between hyperglycaemia, diabetes complications and development of fibrotic conditions among people living with type 1 and type 2 diabetes in England: a retrospective cohort study using UK Clinical Resource Datalink Aurum and Hospital Episode Statistics 2025. BMJ Open. 2025; 15(10): e103426. doi: 10.1136/bmjopen-2025-103426.
9. Teague TT, Payne SR, Kelly BT, Dempsey TM, McCoy RG, Sangaralingham LR, *et al.* Evaluation for clinical benefit of metformin in patients with idiopathic pulmonary fibrosis and type 2 diabetes mellitus: a national claims-based cohort analysis. Respir Res. 2022; 23(1): 91. doi: 10.1186/s12931-022-02001-0.
10. Huo L, Shi W, Chong L, Wang J, Zhang K, Li Y. Asiatic acid inhibits left ventricular remodeling and improves cardiac function in a rat model of myocardial infarction. Exp Ther Med. 2016; 11(1): 57–64.
11. Wang X, Lu Q, Yu DS, Chen YP, Shang J, Zhang LY, *et al.* Asiatic acid mitigates hyperglycemia and reduces islet fibrosis in Goto-Kakizaki rat, a spontaneous type 2 diabetic animal model. Chin J Nat Med. 2015; 13(7): 529–34.
12. Di X, Chen J, Li Y, Wang M, Wei J, Li T, *et al.* Crosstalk between fibroblasts and immunocytes in fibrosis: From molecular mechanisms to clinical trials. Clin Transl Med. 2024; 14: e1545. doi: 10.1002/ctm2.1545.
13. Awaluddin R, Nugrahaningsih DAA, Solikhah EN, Prasetyastuti P. Fibrotic effect of monoculture, conditioned media and coculture of fibroblast NIH3T3 cells on collagen secretion and mRNA TGF-beta expressions. Pharmaciana. 2023; 13: 179. doi: 10.12928/pharmaciana.v13i2.25482.
14. Niu X, Zhang Y, Wang Y. Co-culture models for investigating cellular crosstalk in the glioma microenvironment. Cancer Pathog Ther. 2023; 2(4): 219–30.
15. Holt DJ, Chamberlain LM, Grainger DW. Cell-cell signaling in co-culture of macrophages and fibroblasts. Biomaterials. 2010; 31(36): 9382–94.
16. Hashim P, Sidek H, Helan MHM, Sabery A, Palanisamy UD, Ilham M. Triterpene composition and bioactivities of centella asiatica. Molecules. 2011; 16(2): 1310–22.
17. Toni LS, Garcia AM, Jeffrey DA, Jiang X, Stauffer BL, Miyamoto SD, *et al.* Optimization of phenol-chloroform RNA extraction. MethodsX. 2018; 5: 599–608.
18. Livak KJ, Schmittgen TD. Analysis of relative gene expression data using real-time quantitative PCR and the 2(-Delta Delta C(T)) Method. Methods 2001; 25(4): 402–8.
19. Sousa ESA, Queiroz LAD, Guimarães JPT, Pantoja KC, Barros RS, Epiphanio S, *et al.* The influence of high glucose conditions on macrophages and its effect on the autophagy pathway. Front Immunol. 2023; 14: 1130662. doi: 10.3389/fimmu.2023.1130662.

20. Badillo-Garcia LE, Liu Q, Ziebner K, Balduff M, Sevastyanova T, Schmuttermaier C, *et al.* Hyperglycemia amplifies TLR-mediated inflammatory response of M(IL4) macrophages to dyslipidemic ligands. J Leukoc Biol. 2024; 116(1): 197–204.
21. Panda S, Arora A, Luthra K, Mohan A, Vikram NK, Kumar Gupta N, *et al.* Hyperglycemia modulates M1/M2 macrophage polarization in chronic diabetic patients with pulmonary tuberculosis infection. Immunobiology. 2024; 229(2): 152787. doi: 10.1016/j.imbio.2024.152787.
22. Margaryan S, Poghosyan D, Ghonyan S, Hakobyan L, Martirosyan A, Manukyan G. Long-term hyperglycaemia exerts contrasting effects on M1- and M2-like macrophages. Front Immunol. 2025; 16: 1639650. doi: 10.3389/fimmu.2025.1639650.
23. Negara BFSP, Choi JS. Bifidobacterium lactis inhibits iNOS expression in LPS-stimulated RAW 264.7 macrophages. Indones Biomed J. 2022; 14(2): 199–205.
24. Yu L, Wang R, Hou Q, Yang F, Liu Y, Peng M, et al. Enhanced THBS2 promotes collagen synthesis and inflammatory secretome of fibroblasts in idiopathic pulmonary fibrosis. Sci Rep. 2025; 15(1): 25926. doi: 10.1038/s41598-025-09318-y.
25. Meiliana A, Dewi NM, Wijaya A. Mesenchymal stem cells manage endogenous tissue regeneration. Indones Biomed J. 2016; 8(2): 71–90.
26. Ahmed AB, Chetia P. Selegiline modulates inflammatory indicators in RAW 264.7 macrophages and LPS-aggravated CFA-induced rheumatoid arthritis in rats. Eur J Clin Exp Med. 2024; 22(1): 6–16.
27. Khan S, Wardill HR, Bowen JM. Role of toll-like receptor 4 (TLR4)-mediated interleukin-6 (IL-6) production in chemotherapy-induced mucositis. Cancer Chemother Pharmacol. 2018; 82(1): 31–7.
28. El-Nabarawy N, Gouda A, Shalaby E. Therapeutic intervention of curcumin on interleukin-6 and oxidative stress induced by paraquat toxicity of lung and liver in rats. Biomed Pharmacol J. 2019; 12(4): 1737–48.
29. Altunay C, Yavuz AS, Sozer Tokdemir S. Effect of CXCR9-CXCR3 cytokine signaling pathway in polycytemia vera. Experimed. 2019; 8: 84–92.
30. Biernacka A, Dobaczewski M, Frangogiannis NG. TGF-β signaling in fibrosis. Growth Factors. 2015; 29(5): 196–202.
31. Meng X, Nikolic-paterson DJ, Lan HY. TGF-β: The master regulator of fibrosis. Nat Rev Nephrol. 2016; 12(6): 325–38.
32. Braczkowski MJ, Kufel KM, Kulińska J, Czyż DŁ, Dittmann A, Wiertelak M, *et al.* Pleiotropic action of TGF-beta in physiological and pathological liver conditions. Biomedicines. 2024; 12(4): 925. doi: 10.3390/biomedicines12040925.
33. Shin HY, Kim YS, Ha EJ, Koo JP, Jeong WB, Joung MY, *et al.* Anti-inflammatory action and associated intracellular signaling of Centella asiatica extract on lipopolysaccharide-stimulated RAW 264.7 macrophage. Food Bioscience. 2024; 61: 104614. doi: 10.1016/j.fbio.2024.104614.
34. Yuyun X, Xi C, Qing Y, Lin X, Ke R, Bingwei S. Asiatic acid attenuates lipopolysaccharide-induced injury by suppressing activation of the Notch signaling pathway. Oncotarget. 2018; 9(19): 15036–46.
35. Wu J, Xu G, Zhou X, Wan J, Liao H, Li C, *et al.* Asiatic acid inhibits keloid fibroblast migration and collagen deposition via suppression of STAT3 activation. Burns. 2025; 51(8): 107586. doi: 10.1016/j.burns.2025.107586.
36. Zhu AS, Mustafa T, Connell JP, Grande-Allen KJ. Tumor necrosis factor alpha and interleukin 1 beta suppress myofibroblast activation via nuclear factor kappa B signaling in 3D-cultured mitral valve interstitial cells. Acta Biomaterialia. 2021; 127: 159–68.
37. Aashaq S, Batool A, Mir SA, Beigh MA, Andrabi KI, Shah ZA. TGF-β signaling: A recap of SMAD-independent and SMAD-dependent pathways. J Cell Physiol. 2022; 237(1): 59–85.
38. Xia X, Dai C, Yu HUA, Huang X, Chen ALI, Tan Y, *et al.* Asiatic acid prevents the development of interstitial lung disease in a hypochlorous acid - induced mouse model of scleroderma. Oncology Letters. 2018; 15(6): 8711–6.
39. Awaluddin R, Nugrahaningsih DAA, Solikhah EN, Chabib L. The effect of asiatic acid and metformin on the viability percentage of mouse macrophage cell lines RAW264.7 and mouse fibroblast cell lines NIH3T3. IOP Conference Series: Earth and Environmental Science 2020; 448: 012021. doi: 10.1088/1755-1315/448/1/012021.
40. Liu Y, He K, Hu Y, Guo X, Wang D, Shi W, *et al.* YAP modulates TGF-β1-induced simultaneous apoptosis and EMT through upregulation of the EGF receptor. Sci Rep. 2017; 7: 45523. doi: 10.1038/srep45523.